2024

Smithton Synclinorium 3D model

Author: D. Bombardieri, M. Duffett, M. Latinovic and J. Everard
Date: 29/07/2024
Email: info@mrt.tas.gov.au
Website: www.mrt.tas.gov.au

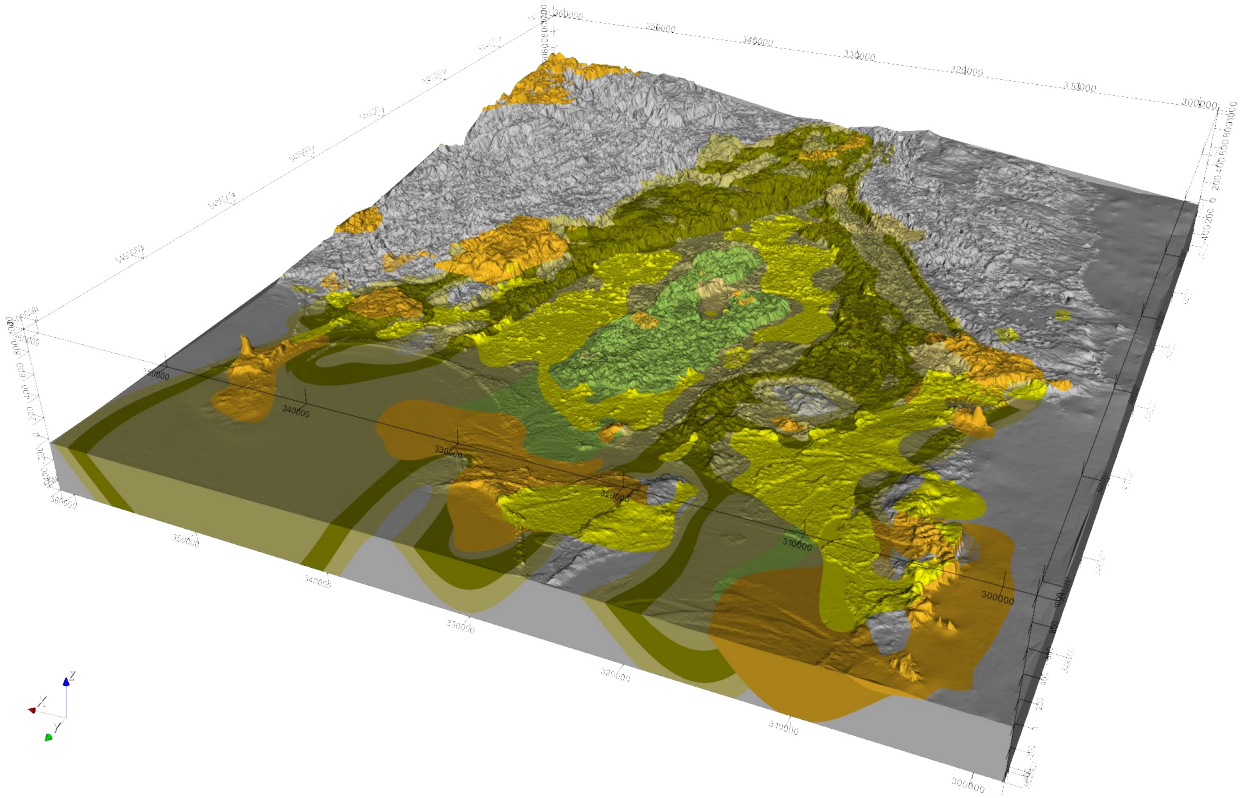

REPORT No.: TR44

Geological Survey Technical Report 44

Tasmanian Government

Geological Survey Technical Report 44:

Smithton Synclinorium 3D model

by

D. Bombardieri, M. Duffett, M. Latinovic and J. Everard

Cover: The Smithton Synclinorium voxet model (voxel cell size, 250 m x 250 m x 10 m) used for volumetric calculations.

Tasmanian Government

Mineral Resources Tasmania www.mrt.tas.gov.au Department of State Growth

Smithton Synclinorium 3D model

by D. Bombardieri[1], M. Duffett[1], M. Latinovic[2] and J. Everard[1]
[1]*Geological Survey Branch - Mineral Resources Tasmania*
[2]*Department of Natural Resources and the Environment*

CONTENTS

FIGURES

1.0 INTRODUCTION

The Smithton Synclinorium 3D geological model has been developed as part of the Tasmanian Groundwater Assessment Project (GAP) and is a key step to understanding the groundwater resource in this region. Its primary focus is to determine the 3D geometry of geologic units that host potential groundwater resources.

The GAP is one of three 'Water Science' projects funded by the Tasmanian Government and the Australian Government's National Water Grid Fund (NWGF) that are underpinning our knowledge base and supporting a range of actions under the Tasmanian Government's Rural Water Use Strategy (RWUS) (DPIPWE, 2021). The GAP directly supports the delivery of Action 1.2 of the strategy to consider any knowledge gaps identified through the ongoing Groundwater Risk Assessment and Management Framework project and identify actions to improve our management of groundwater resources.

This technical report provides a summary of the methodology used to create the Smithton Synclinorium 3D geological model. The software employed (3D GeoModeller™) computes 3D models directly from outcrop and drillhole geological observations, supplemented where necessary by inferred and interpreted contacts and structures. The 3D objects produced from this study will be used in hydrological flow modelling applications to improve our understanding of the groundwater water balance for this region.

2.0 TECTONIC AND GEOLOGICAL SETTING

The Smithton Synclinorium, located in far north-west Tasmania (Figure 1), is a complex structure resulting from Proterozoic extension and Palaeozoic compression of two Proterozoic sequences. The oldest exposed component, the Mesoproterozoic Rocky Cape Group (Halpin et al., 2014) is a dominantly siliciclastic shelf sequence, which also flanks the Synclinorium to the east and west. It is overlain within the Synclinorium by the Neoproterozoic to Early Cambrian Togari Group (Everard et al., 1996, 2007; Calver, 1998), a volcano-sedimentary marine shelf and rift sequence of dominantly dolostone, mafic volcanics and siliciclastics. The base of the Togari Group rests unconformably on different units of the Rocky Cape Group basement. Overlying the Togari Group in the axis of the Synclinorium is Middle to Late Cambrian mudstone and lithic sandstone of the Scopus Formation, defined by Everard et al. (2007, p. 100); previously it was informally known as the Christmas Hills sequence and described by Baillie in the Smithton Explanatory Notes (Brown et al., 1989, p. 26).

Two early phases of syn-depositional extension were followed by at least four compressional phases of deformation, the latter probably in both Cambrian and Devonian times. The broadly triangular outline of the Synclinorium in plan is a consequence of these contrasting NNE- and NW-trending fold generations.

Metamorphism in the Rocky Cape Group ranges from very low (prehnite-pumpellyite facies) to low (greenschist facies) grade, with local development of garnet and andalusite outside the current study area. Dating of monazite inclusions in andalusite porphyroblasts indicate a metamorphic event at ~1100 Ma (Cumming et al., 2024). However, metamorphic assemblages in the Spinks Creek Volcanics (~580 Ma) also indicate prehnite-pumpellyite to locally greenschist facies metamorphism, presumably of either Cambrian or Devonian age.

Syn-depositional extension has been recognised in the Rocky Cape Group and was very important during deposition of the Togari Group. In particular, the Roger River Fault, a major NNE-trending, west-side down structure transecting the Synclinorium (Figure 2), was probably initiated as a growth fault, resulting in large Togari Group unit thickness changes (Everard et al., 2007).

Permian sediments are volumetrically insignificant in the model area, occurring only as thin outliers of the Tasmania Basin in the extreme south-eastern corner.

Younger units encompass Paleogene-Neogene basalts and unconsolidated Cainozoic sediments. Towards the top of this sequence is late Pleistocene marine sand and gravel which fringes the coastline and extends about ten kilometres inland in low lying areas. These deposits grade inland and upwards into aeolian sand. Close to the present shoreline the Pleistocene deposits are overlain by younger beach and aeolian sand deposits. Pleistocene to Holocene alluvium and some swamp deposits occupy the river valleys and are particularly well developed over the low relief topography developed on the dolostone units within the Togari Group (Everard et al., 2007).

2.1 Lithostratigraphy

The geological units modelled and characteristics relevant to their representation in three dimensions are outlined briefly herein. Everard et al. (2007) should be referred to for full descriptions. The alphabetical lithostratigraphic unit codes employed as a shorthand representation in this section and throughout are those used in MRT's 1:250,000-scale mapping.

2.1.1 Rocky Cape Group (Lrj, Lri, Lrd, Lrc, Lrb. Lrl, Lrp)

The Mesoproterozoic Rocky Cape Group is estimated to be >10 km thick (Mulder et al., 2015), consisting almost entirely of quartz arenite, siltstone, and mudstone, deformed and metamorphosed at prehnite-pumpellyite to lower greenschist facies conditions (Halpin et al., 2014). For the purposes of this project, several Rocky Cape Group units were combined and modelled as a single basement unit. These include the Jacob Quartzite (Lrj), Irby Siltstone (Lri), Detention Group (Lrd), Cowrie Siltstone (Lrc), Balfour Subgroup (Lrb) Lagoon River Quartzite (Lrl) and Pedder River Siltstone (Lrp).

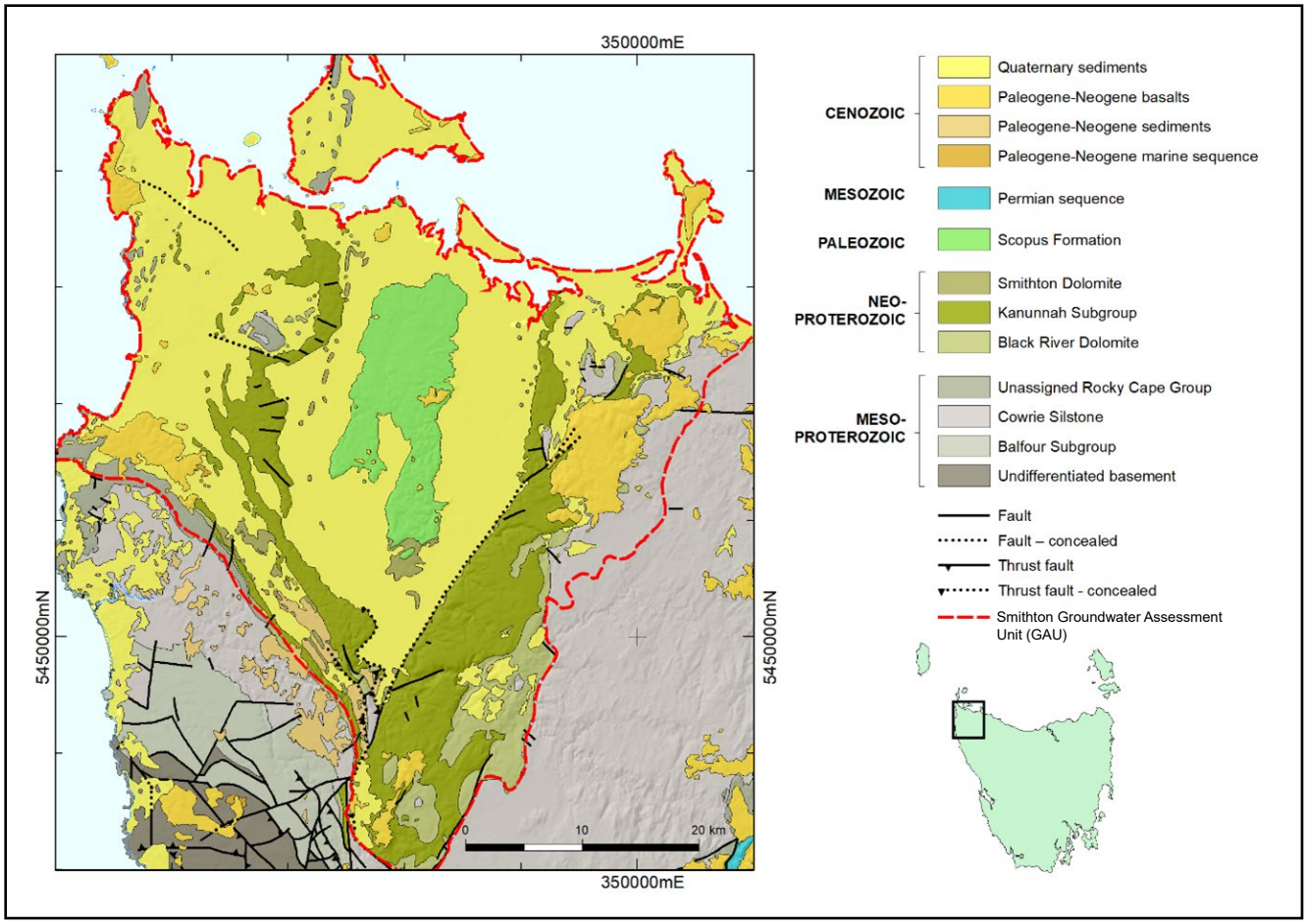

Figure 1. (Above) Smithton Synclinorium study area.

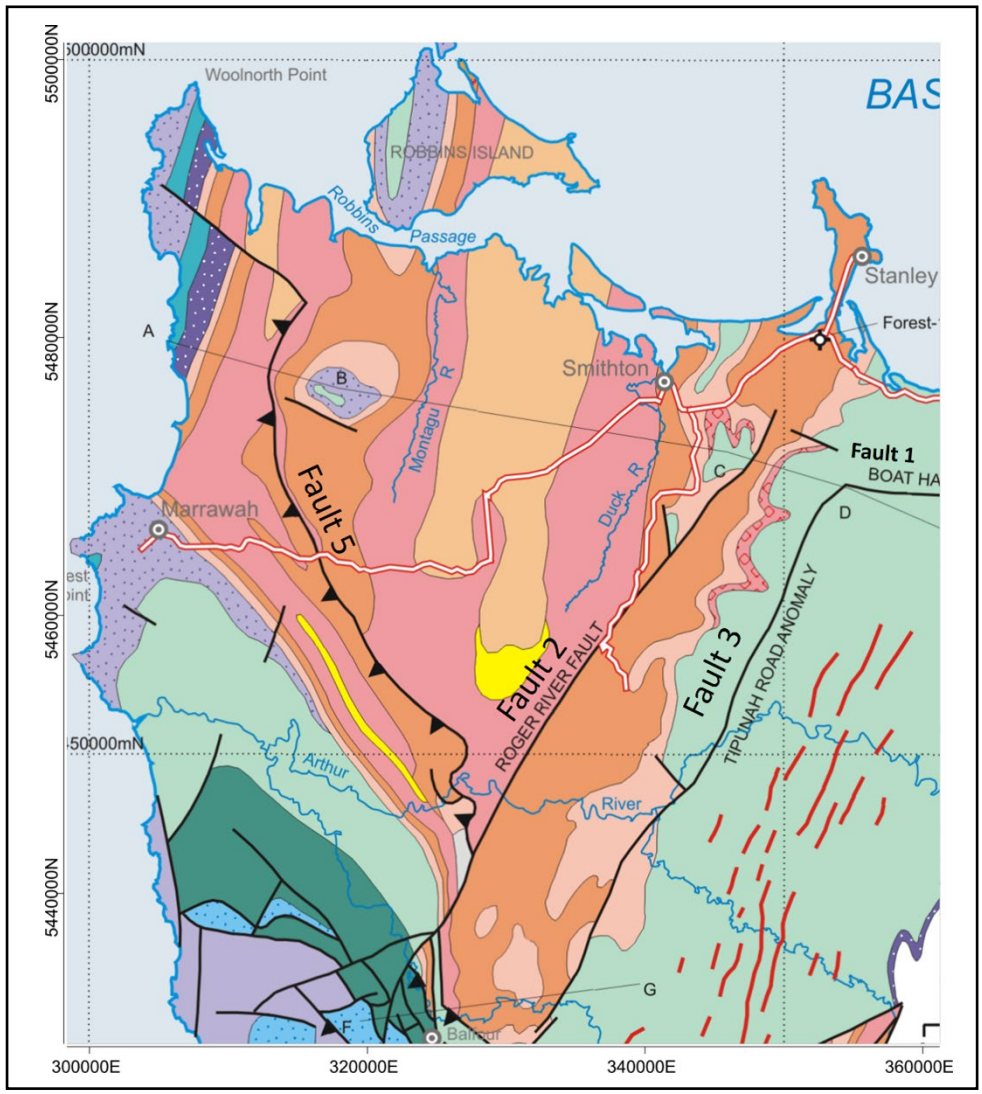

Figure 2. (Left) The major faults structures of the Smithton Synclinorium. See Calver et al. (2014) for geological nomenclature.

2.1.2 Togari Group

The mostly Neoproterozoic Togari Group overlies the Rocky Cape Group with angular unconformity. It is here treated as four main lithostratigraphic units, based on Everard et al. (2007) and Mulder et al. (2020).

The Black River Dolomite (Mulder et al., 2020; Lss) consists of up to 800 m of Tonian interbedded shallow marine dolostone, black shale and chert, with dolomitic diamictite near the top. The unit is, however, markedly thinner (~280 m) on the western side of the Synclinorium. It is locally underlain by an impersistent basal siliciclastic unit up to 120 m thick, the Forest Conglomerate. In many places, however, the Forest Conglomerate is absent and the Black River Dolomite rests directly on Rocky Cape Group basement. Accordingly, the Forest Conglomerate has been incorporated with the Black River Dolomite for modelling purposes.

The Kanunnah Subgroup (Lsv, Lsb) is a Cryogenian-Ediacaran volcano-sedimentary unit up to 1400 m thick east of the Roger River Fault, but locally only 220 m thick west of it. Three interdigitating formations have been identified. The Keppel Creek Formation consists of volcaniclastic lithic wacke sandstone and siltstone, with subordinate conglomerate, mudstone, limestone, dolostone and ironstone. The Croles Hill Diamictite contains clasts of basalt and sedimentary rocks and occurs as lenses within the Keppel Creek Formation. These units are typically overlain by massive to occasionally pillowed tholeiitic basalt, the Spinks Creek Volcanics, which may in turn be overlain by more volcaniclastics. Due to the laterally discontinuous nature of its constituents, despite recent recognition of significant time breaks within it (Mulder et al., 2020), the Kanunnah Subgroup has been modelled as a single unit.

The Smithton Dolomite (Lsd) is an Ediacaran shallow marine carbonate, approximately 1,500 m thick. The lower 500 m consists of dolomicrite and oolitic dolograinstone, with massive crystalline dolostone comprising the upper 1,000 m (Calver, 1998).

The Salmon River Siltstone consists of up to ~350 m of thinly bedded siliceous siltstone and shale, with sparse Early to Middle Cambrian fossils. Due to limited exposure, and discontinuous nature it was included with the unconformably overlying, but structurally concordant, (Everard et al., 2007) Scopus Formation. Open, upright folds in this formation also affect the underlying Salmon River Siltstone and other Togari Group units (Everard et al., 1997, p. 128).

2.1.3 Scopus Formation (Cm)

The late Middle to early Late Cambrian Scopus Formation, which lies in the core of the Smithton Synclinorium, is composed of thin to thick-bedded, coarse to fine-grained lithic wacke sandstone, granule conglomerate, siltstone and mudstone (Everard et al., 2007).

The formation is estimated to be approximately 300 m thick (Corbett et al., 2014), however this is not well defined and this thickness must be regarded as a minimum.

2.1.4 Paleogene-Neogene sediments and marine sequence (Ts and Tm)

Cenozoic sediments comprise poorly consolidated freshwater (Ts) and marine sediments (Tm). These have been modelled as separate elements based mainly on borehole log data. Early Miocene limestone occurs at Redpa, Marrawah and Cape Grim (Quilty, 1972), underlying basalt at Redpa and around Woolnorth. In the Montagu area and on eastern Robbins Island these units are concealed by both basalt and younger sediments and have been modelled using information from water bores. Only Ts freshwater sediments are present in the east of the study area, generally in association with Cenozoic basalts.

Thin occurrences of freshwater sediments (<15 m thick) are known in the southern part of the study area (Salmon River and Blackwater Rivulet) but are only partially represented in the model where both thickness and drill/pit hole data density are sufficient.

2.1.5 Paleogene-Neogene basaltic rocks and clays (Tb)

In the study area, Cenozoic basalt (Tb) occurs mostly as thin hill cappings, with major areas around Marrawah, Forest, Lileah and near Balfour. These basalts are probably the dissected remnants of an extensive series of flows that once covered much of the region (Everard et al., 2007). Basalts can be separated by interbedded layers of sandy sediments and can be deeply weathered to clays at surface exposures (DPIPWE, 2012). This lithological variation has not been included in the final model due to its highly discontinuous nature and uncertainty of its distinction in the primary data sets.

2.1.6 Quaternary sediments (Qh, Qps)

Quaternary sediments can be divided into coastal marine sediments and alluvial/aeolian complexes. Thicknesses of coastal marine sediments are variable, normally ranging from 2 m to 10 m with maximum depths of up to 30 m. The alluvial/aeolian complexes tend to be thicker, more often closer to 30 m (DPIPWE, 2012). Most are developed on, or closely associated with, poorly outcropping Smithton Dolomite bedrock. Extensive similar deposits also overlie the Black River Dolomite (Everard et al., 2007).

Despite these differences, in this study it was practically necessary to treat the Quaternary sediments as a single element, as they were very thin in comparison to the total model extent. Quaternary sediments have not been modelled outside of the Smithton groundwater assessment unit (GAU) boundary (Figure 1).

2.1.7 Faults and dykes

Only major faults, that is, structures observed to significantly displace geological units on a regional scale, are represented in the modelling and are illustrated in Figure 2.

The NNE-trending Roger River Fault, Fault 2 in the model, is the largest fault observed in the study area. It is steeply dipping with ~750 m of west-side-down net offset. Differences in the thickness of Togari Group units on either side, however, suggest that it originated as an east-side-down extensional fault which formed the western boundary of a half-graben during deposition of the Togari Group volcano-sedimentary sequence. Reactivation and dextral transgression during Cambrian and/or Devonian compressional episodes resulted in the existing geometry (Everard et al., 2007). Towards the south of the Synclinorium, the Roger River Fault branches into multiple splays that are linked to the NNW-trending Balfour Shear Zone within the Rocky Cape Group.

The Boat Harbour Fault is a major east-west trending dextral wrench fault within the Rocky Cape Group, in the east of the study area, with a horizontal displacement of ~8 km near Boat Harbour (Gee, 1971). Although it post-dates regional folds and cleavage in the Rocky Cape Group, it appears to terminate east of the Smithton Synclinorium, without offsetting Togari Group units therein (Seymour, 1997).

Fault 3 is a NNE-trending structure, subparallel to the Roger River Fault but about 10 km further east. It transects both the Rocky Cape Group and Togari Group, and locally forms the boundary between them with west-side down net movement of perhaps ~500 m. Although, unlike the Roger River Fault, it has little topographic expression, it coincides with a strong linear magnetic anomaly. Seymour (1997) suggested that this "Tipunah Road Anomaly" may have originated as an east-directed thrust, or represent one of several similar thrusts, that took up the movement on the Boat Harbour Fault.

Fault 5 is a major inferred NW trending, NE-directed thrust fault within the Togari Group, interpreted from magnetic data by Calver et al. (2014) and Halpin et al. (2014).

Aeromagnetic imagery of far northwest Tasmania (Figure 3) shows a series of parallel, WNW-ESE-trending linear magnetic anomalies most prominent between Smithton and Montagu. The anomalies crosscut several major structures including the Roger River Fault. Several of these narrow (several metres) alkali dolerite dykes are exposed in a quarry at Smithton, northwest Tasmania. Ar-Ar dating indicates a mid-Cretaceous age (Everard and Bottrill, 2023).

2.2 Hydrogeology

2.2.1 Previous Investigations

Gulline (1959) studied the Smithton GAU's groundwater potential. From 1999 to 2006, Matthews and Donaldson (1999), Latinovic (2002), and Matthews and Donaldson (2006 a and b) created state groundwater maps, identifying significant groundwater development at Mella and Togari in the "Main Smithton Dolomite Aquifer".

The hydrogeological investigation conducted by Harrington (2008), and Harrington and Currie (2008a, b), synthesized the previously available groundwater information and additional data gathered during the field investigation stage of the Tasmanian groundwater modelling project. Harrington (2008), and Harrington and Currie (2008a, b), prepared preliminary conceptual water balances for the Smithton Syncline Groundwater Management Unit (GMU), as well as for the Mella and Togari areas, as part of their projects. Subsequently, a combined numerical model for the Mella–Togari area was developed, which incorporated additional water balance components that were not determined in the initial conceptual reports (Stadder, 2009).

Harrington et al. (2009) reported the results of the groundwater assessment and modelling components of the CSIRO Tasmania Sustainable Yields projects. This assessment is largely based on the results of the aforementioned 2008-2009 reports. The presented results indicate that recharge rates under all future climate scenarios are likely to be similar to the recharge rates experienced during the historical period (1924-2007).

Rockliff and Sheldon (2011) explored the proposed Smithton GMU's hydrogeology, focusing on aquifer and surface water connectivity. They reviewed the area's land use, climate, water use, and ecological values, confirming the "Main Smithton Dolomite Aquifer" as the primary water source.

Recent findings from the "Groundwater Risk Assessment and Management Framework" project (NRE Tas, 2024) revealed that among the 32 newly developed State Groundwater Assessment Units (GAUs), the Smithton Syncline GAU faces the highest risk of overuse. To enhance understanding of the geological architecture supporting groundwater resources in this crucial agricultural region, the development of a 3D geological model was recommended.

2.2.2 Hydrogeological Summary

The Smithton Groundwater Assessment Unit (GAU) harbours a significant, yet not fully quantified, groundwater resource. This resource is found within a variety of unconsolidated sediments, sedimentary metamorphic rocks, and fractured igneous units. Among these, the unconsolidated aquifers, which are characterized by intergranular porosity, are primarily located in Quaternary and Paleogene-Neogene sediments and serve as important sources of water. In addition to these, there are fractured aquifers that occur in Proterozoic dolomites, Cambrian rocks of the Scopus Formation, and distinct Paleogene-Neogene basalt occurrences. These fractured aquifers also contribute significantly to the overall availability of groundwater. Thus, both unconsolidated and fractured aquifers together host the vital groundwater resource of the Smithton GAU.

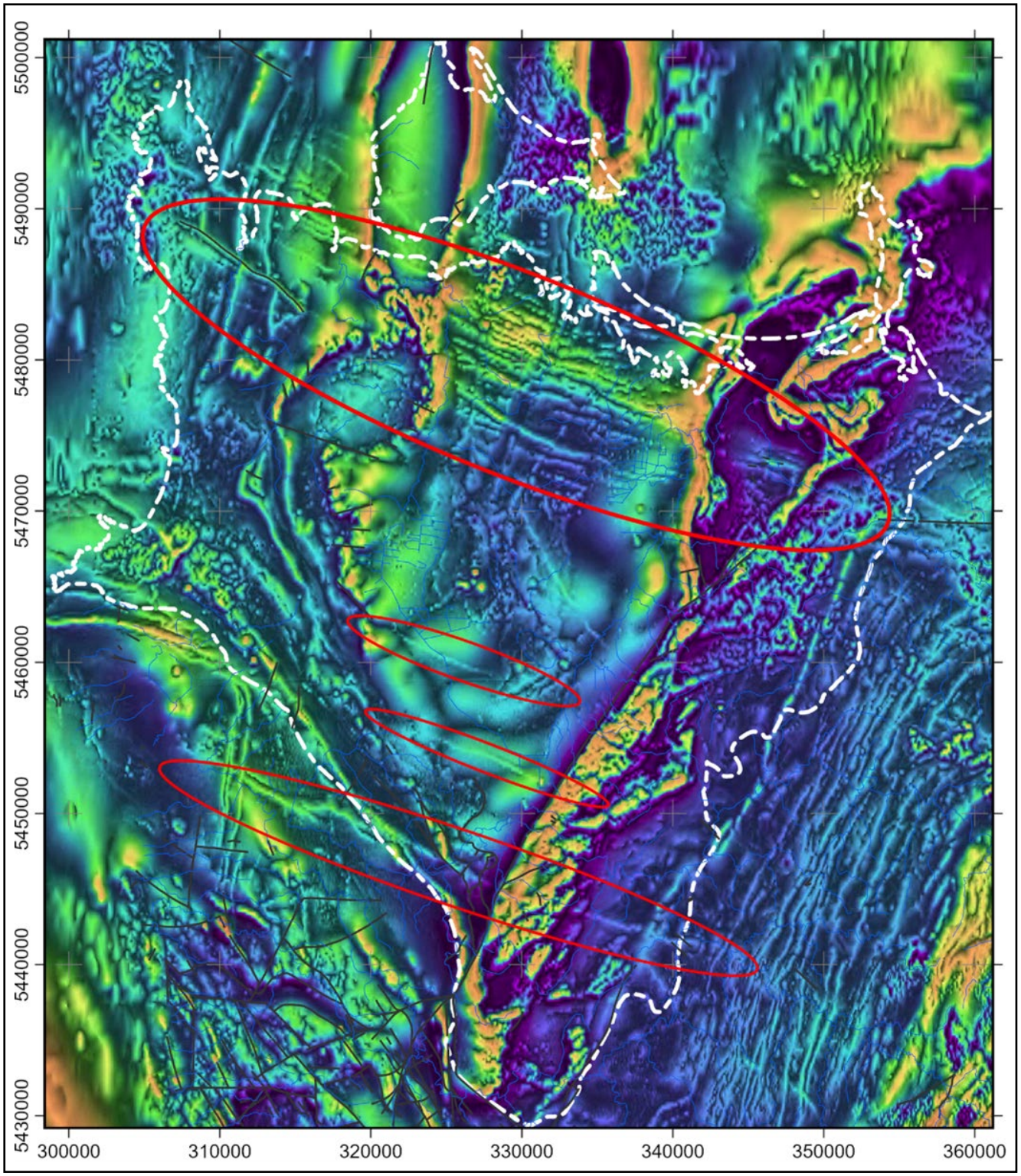

Figure 3. Total Magnetic Intensity image of the study area. Red ellipses highlight WNW-ESE trending linear magnetic features interpreted to represent dykes.

A comprehensive list of the main known aquifers in the area is provided in the Tasmanian Aquifer Framework (DPIPWE, 2012). Table 1 displays the recorded well yields, salinities, and bore depths from the GWIMS database for water wells within the Smithton GAU.

Regional groundwater flow within the Smithton syncline area, encompassing the Welcome, Montagu, and Duck River catchments, predominantly occurs northward (as documented by Harrington (2008) and Stadder (2009)). Notably, the majority of high-yield boreholes are associated with the Smithton and Black River Dolomite aquifers (Table 1).

Historically, the largest number of water bores were drilled in the Smithton Dolomite aquifers that occur at shallow depths in the middle and lower reaches of all major river catchments (Duck, Montagu and Welcome). These coincide with areas of major agricultural and dairy activities.

In comparison, Black River Dolomite aquifers are only easily accessible and targeted with shallow bores along the eastern edge for drilling. In the remainder of the Smithton GAU, they are located at depths in excess of 200 m (except Dismal Swamp and upper reaches of Harcus River).

Lithostratigraphy	Bore holes (n)	Bore Yields (litres/sec)		Salinity (mg/L)		Bore Depth (m)	
	Total	**Range**	**Average/ Median**	**Range**	**Average/ Median**	**Range**	**Average/ Median**
Quaternary Sediments - Qha	33	0.06 – 20.20 (24)	1.84 / 0.38	463 - 3,098 (5)	1,255 / 1,033	4 - 54 (33)	18 / 17
Paleogene Neogene basaltic rocks - Tb	239	0.05 - 35.00 (177)	1.75 / 0.60	90 - 3,500 (31)	535 / 350	5 - 126 (239)	38 / 32
Paleogene Neogene marine sequence - Tm	11	0.60 - 37.88 (11)	10.90 / 8.00	240 / 1,200 (9)	696 / 570	15 - 60 (11)	37 / 37
Paleogene Neogene sequence sediments - Tsgs	44	0.25 - 12.63 (35)	2.60 / 0.50	90 - 1,300 (5)	592 / 616	11 - 120 (44)	29 / 25
Scopus Formation - Cm	185	0.05 - 30.31 (156)	3.23 / 0.63	130 - 1,990 (36)	812 / 718	4 - 150 (182)	47 / 37
Smithton Dolomite - Lsd	400	0.01 - 52.53 (327)	10.70 / 8.70	233 - 7,500 (84)	747 / 565	4 - 120 (400)	36 / 30
Kanunnah Subgroub - Lsvw, Lsv, Lsb	Lsv 240 + Lsb 30	0.03 - 50.00 (239)	3.70 / 1.26	70 - 4,800 (46)	436 / 275	7 - 138 (268)	50 / 43
Black River Dolomite - Lss, Lscb	63	0.03 - 25.00 (52)	4.50 / 1.80	90 - 588 (8)	332 / 333	12 - 96 (63)	40 / 37
Rocky Cape Group - Lrj, Lri, Lrd, Lrc, Lrb, Lrl, Lrp	56	0.06 - 17.00 (50)	2.34 / 0.63	95 - 910 (10)	304 / 255	14 - 186 (56)	50 / 40

Table 1. Parentheses indicate the number of bore holes use to calculate statistics.

Regionally, the Kanunnah Subgroup separates the Smithton and Black River Dolomites. However, along the Roger River fault (Fault 2, Figure 2), in places where these lithologies are in direct contact, groundwater flows from the elevated Black River Dolomite toward the main Smithton Dolomite. Additionally, a line of springs along this fault, coupled with the less permeable Kanunnah Subgroup, contributes to groundwater discharge (as observed by Rockliff and Sheldon, 2011).

Most bores in the Kanunnah Subgroup were drilled in sedimentary sequences with yields ranging from 3 to 50 litres/sec (Table 1). Just eleven percent were drilled in the Kanunnah Subgroup basalt as the unit has low permeability due to its composition and may be considered an aquitard.

Aquifers and associated boreholes occur in Proterozoic, Cambrian, and Paleogene-Neogene basalt lithologies. In regions with high borehole density (such as Mella, Togari, Forest, Redpa, Woolnorth, and Montagu), groundwater plays a crucial role for various purposes (dairy farming, agriculture, and domestic use).

Historically, bores drilled in the Mesoproterozoic Rocky Cape Group were seldom used for irrigation due to their location on the outskirts of the Smithton GAU, beyond the primary agricultural and dairy region of the Smithton Basin. However, recent groundwater exploration has identified productive boreholes in the lower reaches of Welcome River, Harcus Creek, and further south near Marrawah. Additionally, high-yield irrigation bores were drilled along the eastern boundary of the study area (e.g., the Gibson Plains).

Despite limited groundwater development, the exact contribution of these boreholes to the overall basin water balance remains uncertain. Recent bore data from the Port Latta area suggests groundwater yields comparable to those of the Kanunnah Subgroup and Scopus Formation (Table 1).

The region between Montagu and Scopus is known for hosting the most productive part of the Scopus Formation, with bore yields reported to be up to 30 litres/sec. However, the groundwater flow in this region may be impacted by Cretaceous dyke swarms, which are characterised by their low permeability. It is noteworthy that the mound springs and artesian bores in the Mella area align spatially with the NW-SE trending dolerite dykes. These dykes seem to have a damming effect, pressurizing water at depth and exploiting existing rock weaknesses, as observed by Rockliff and Sheldon (2011). Furthermore, an analysis of water level data during this study reveals an interesting phenomenon. The water levels up-gradient from the dykes are approximately 5 m higher than those down-gradient, indicating the significant impact of these geological features on the region's hydrology.

An analysis of geological, geomorphological, and hydrogeological data suggests that a comparable structural control mechanism on groundwater flow direction may exist in the Woolnorth area. Specifically, the presence of the Welcome River Marsh could be associated with the occurrence of Cretaceous dolerite dykes and the regional fault structure (Fault 5, as shown in Figures 2 and 3).

Paleogene-Neogene basalts, which overlay older aquifers, serve as a reliable water source for livestock and domestic use. High-yield boreholes within these basalts occasionally facilitate direct irrigation. Typically, younger Quaternary units cover Paleogene-Neogene sediments and marine limestone sequences (Ts and Tm). Aquifers in the Paleogene-Neogene sediment (Ts) units generally yield lower averages compared to marine limestone aquifers (Table 1).

Quaternary deposits host localised aquifers. Impervious layers within these alluvial deposits create perched water tables (Gulline, 1959). Despite their smaller volume, these groundwater resources significantly contribute to recharging the underlying dolomite aquifers and supporting ecosystems.

Most of the groundwater bores in the Smithton GAU area produce water with a salinity level suitable for various purposes, including commercial irrigation, livestock, and domestic use. A highly saline zone, with a salinity of up to 17,500 mg/L, is present in a portion of the marine limestone aquifer at Woolnorth (DPIPWE, 2012). The highest salinity recorded in the Smithton Dolomite, 7,500 mg/L, is found in a bore located beneath the aforementioned saline zone, indicating the mixing of water from two aquifers.

Results from Table 1 indicate that the Smithton Dolomite (Lsd) and Paleogene-Neogene basalts (Tb) are the primary drilling targets for groundwater resources in the Smithton Groundwater Assessment Unit (GAU). Several factors contribute to this preference, with shallow aquifers in agricultural areas being the key factor. Following these, the Kanunnah Group and Scopus Formation exhibit increased mean bore depths. However, the Black River Dolomite remains largely unused due to its limited known exposure at shallow depths.

3.0 METHODOLOGY

The Smithton Synclinorium 3D model was constructed in GeoModeller™ by constructing geological surfaces or volumes, mostly without explicitly defining them. This approach computes surfaces bounding model unit volumes directly from geological observations (stratigraphic contacts and structural measurements). These are used to define a mathematical potential field in 3D space, for each coherent geological sequence (series) in the model stratigraphic pile (Figure 4). From this potential field, iso-surfaces are taken to define boundaries of the geological units represented in the pile (McInerney et al., 2005).

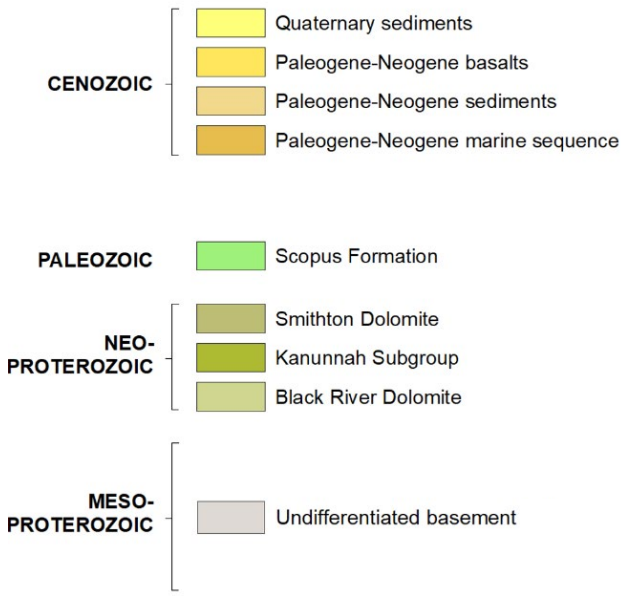

Figure 4. 3D model stratigraphic pile.

3.2 Model construction

A 60 x 70 km subset of a digital elevation model (DEM) with cell size 120 x 120 m (Figure 5; Beaman, 2022) was used as the starting mesh, defining the model's horizontal extent. The depth extent chosen, 500 m, is small in comparison to the modelled area but nevertheless selected in order to better enable model resolution of thin units. Furthermore, we chose 500 m as it is a practical lower limit for groundwater resources.

The 3D geological model is primarily based on MRT's 1:250,000 geological map (Calver et al., 2023) but also incorporated elements of the Calver et al. (2014) mapping, particularly where this interpreted pre-Cenozoic geology lies beneath the younger cover. These maps were used in digitising geological boundaries and fault traces on the DEM surface. Observed and interpreted structural data (dip/strikes) were imported from MRT's structural observations database.

Geological unit contact data at depth were imported from the Tasmanian Groundwater Management Information System (GWIMS), a drilling database containing information for 1,080 water bores in the model area (Figure 6). Stratigraphic attributes in terms of 1:250,000 geological mapping units were interpreted from lithological log data associated with these bores, which is mainly sourced from driller logs. To this was added stratigraphic unit intercept information recorded for 372 drillholes and pits in MRT's drilling database.

From these primary data sets, initial models were calculated. Once computed, they can be rendered in 2D (section profiles) and 3D (surfaces), thus enabling visualisation of model fit against outcrop observations and drillhole intersections. These were then refined in an iterative process, informed by and thus synthesising earlier interpretations, particularly Everard et al. (2007), DPIPWE (2012) and elements of the Statewide 3D geological model (Murphy et al., 2004; Bombardieri et al., 2023; Bombardieri and Duffett, 2023). From these and additional interpretations made in the preliminary stages of this project, a total of 19 interpretive sections with variable spacing and orientation were taken for modelling (Figure 7). Where warranted, additional constraint ('model constructor') points were placed at depth on these sections to guide the potential field interpolator towards plausible structural geometries. In volumes where data or previous interpretation was sparse, further computed model sections were created and similarly used to guide the model calculation. This process is illustrated in the following section.

For model output, a voxel resolution of 250 m x 250 m x 10 m was chosen as optimising resolution while retaining practical computational speed.

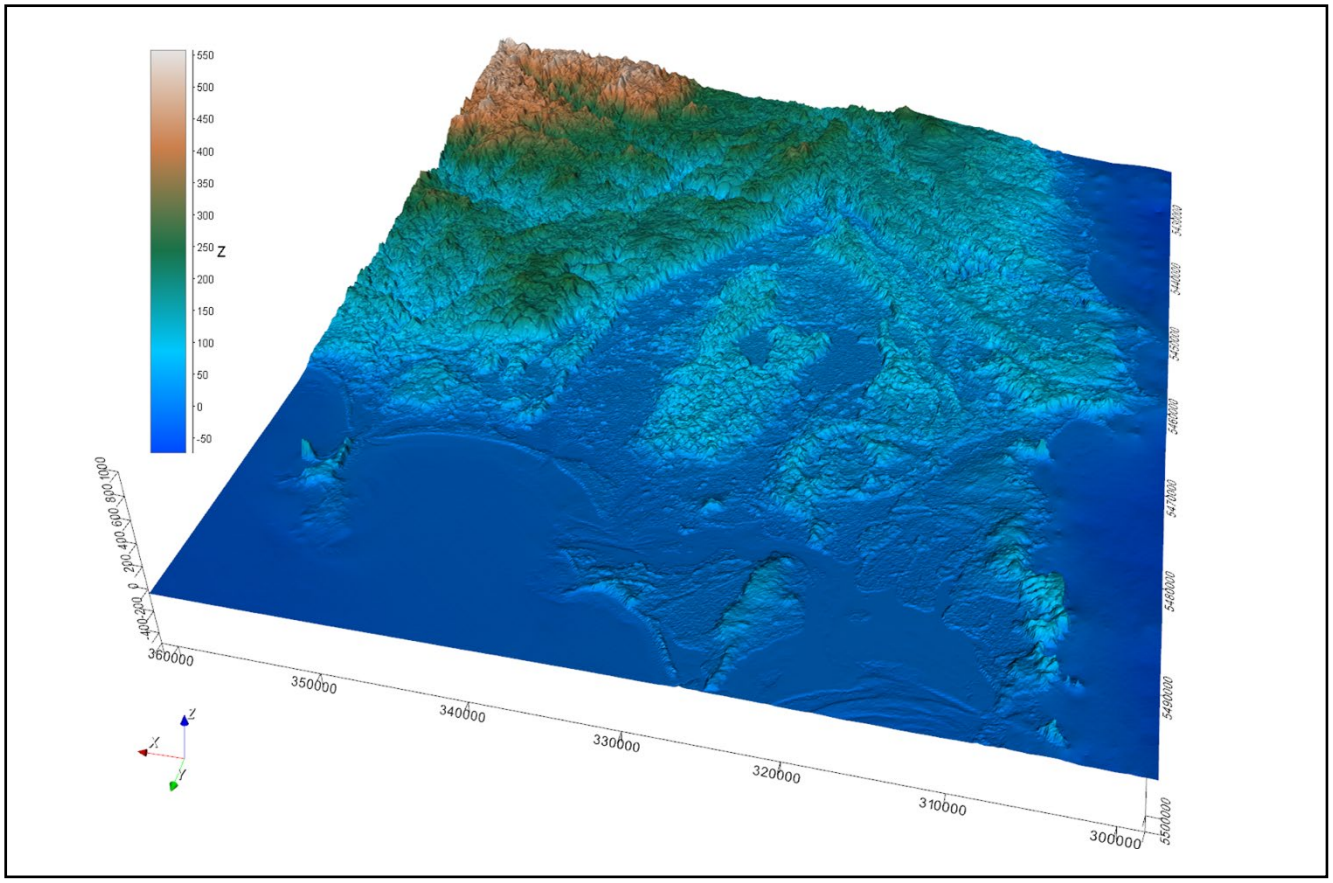

Figure 5. (Above) Digital elevation model of the study area illustrated in 3D with cell size at 250 m x 250 m.

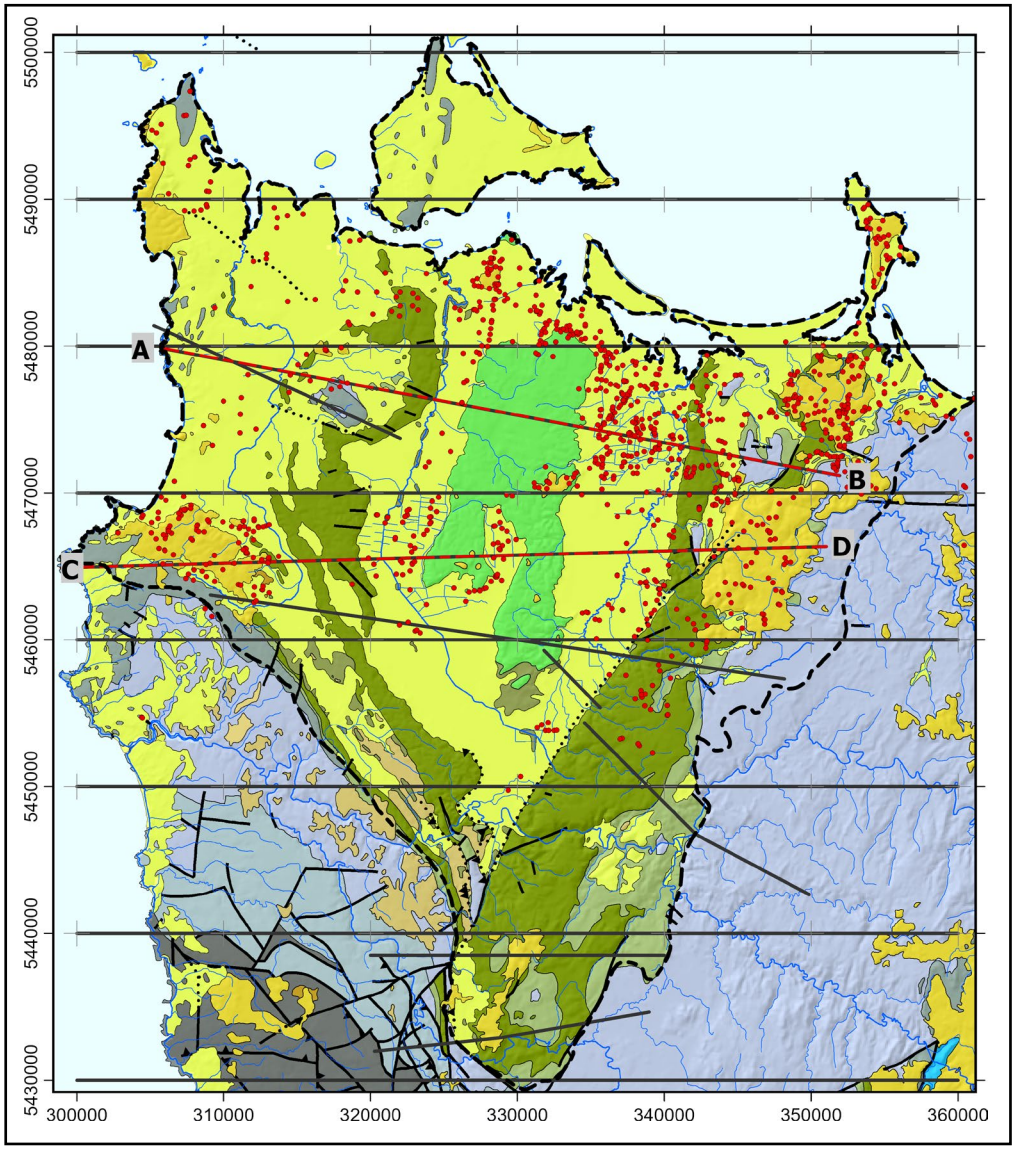

Figure 6. (Left) Nineteen interpretive sections (black and red lines) and bore holes (red dots) used for model construction.

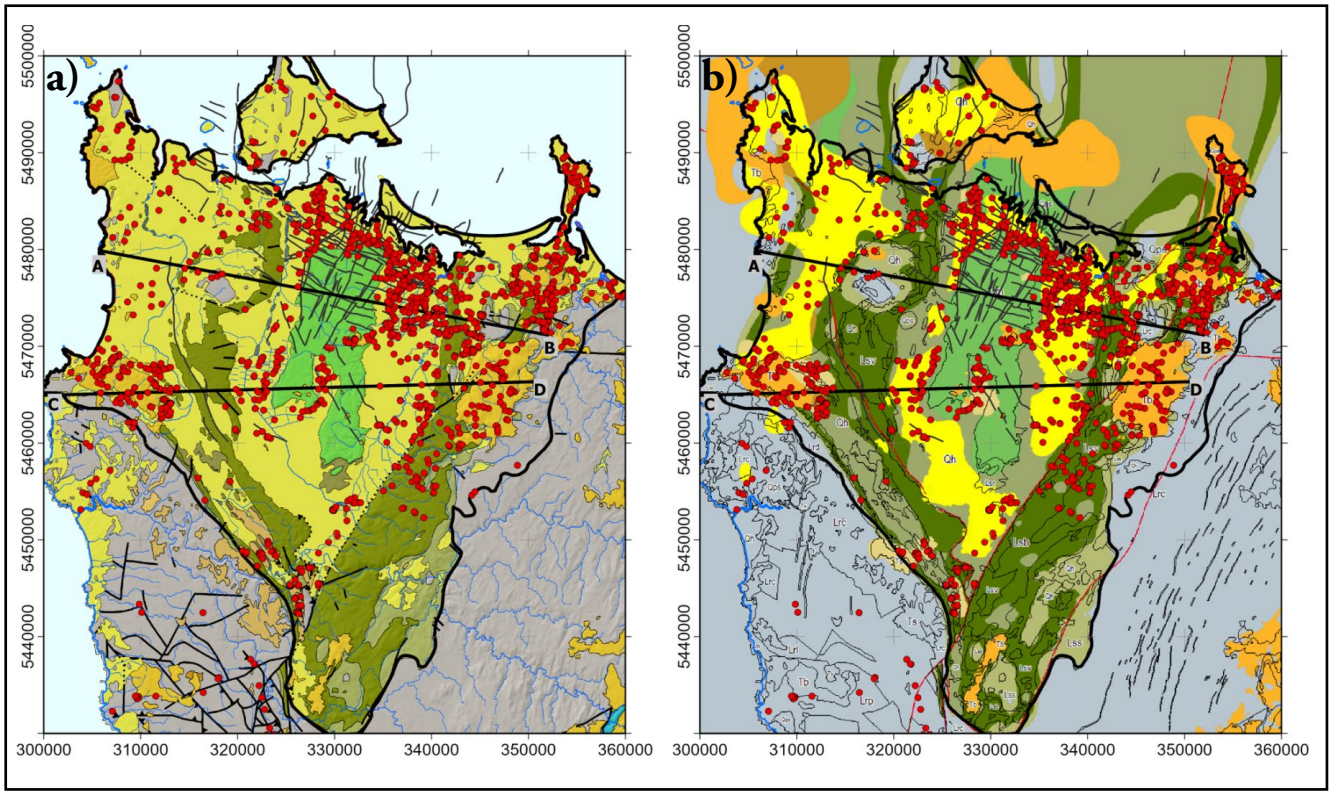

Figure 7. a) represents the mapped geology of the study area, and b) represents the computed model geology.

4.0 RESULTS AND DISCUSSION

4.1 Modelling Results

The model's consistency was evaluated by comparing output results with known geology as represented in maps, together with selected boreholes and two representative sections. Broad correspondence is observed (Figures 7a and 7b). However, Quaternary sediments are notably less extensive in the model than depicted in 1:250,000 mapping. This is generally attributable to this layer becoming too thin for the model to resolve, particularly when extrapolating to areas where borehole data are sparse. Borehole intercepts show the Quaternary to be only a few metres thick in many areas where it has been mapped, thus the volumetric representation of this unit in the model is not considered to be significantly affected. Across the study area, the median thickness of Quaternary sediments intersected is 16.8 m.

Results for the remaining, more voluminous model units appear consistent with available observations and plausible geological inferences, throughout the model space.

Following is an illustration of this outcome, the regional structure and the modelling process in detail, via two representative sections.

4.1.1 Section A-B_ SmithtonProfile

Section A-B (Figure 8) traverses the northern part of the Smithton Synclinorium, extending from Calm Bay to the vicinity of Irishtown (refer to Figure 7). This section intersects four boreholes linked to the catchments of the Welcome, Montagu, and Duck Rivers, inclusive of a borehole drilled in Sedgy Creek.

A close correlation is observed between the interpretive geological section and the computed geological section, with the main regional fold structures largely reproduced. The faults (indicated by red dashed lines) in the computed geological section are somewhat steeper compared to the reference section, a result of reinterpretation during modelling.

Figure 8 also compares borehole logs and the computed geological model. For boreholes 61041414 (A), 61000263 (B) and 61030264 (D), the difference is negligible, a few metres or less of Quaternary sediments. The discrepancy in base of Quaternary for borehole 61031229 (C) is less than 10 metres, considered acceptable given the model scale.

4.1.2 Section C-D_ SmithtonProfile

Section C-D (Figure 9) passes west-east through the Smithton Synclinorium south of Christmas Hills and intersects bore holes associated with the Welcome River, Montagu River and Duck River catchments. The Paleogene-Neogene basaltic unit is present on this section.

Generally, there is good agreement between the interpretive and computed geology section with the regional fold structures reproduced. The overall geometry is similar to Section A-B which is located 5-15 km northward

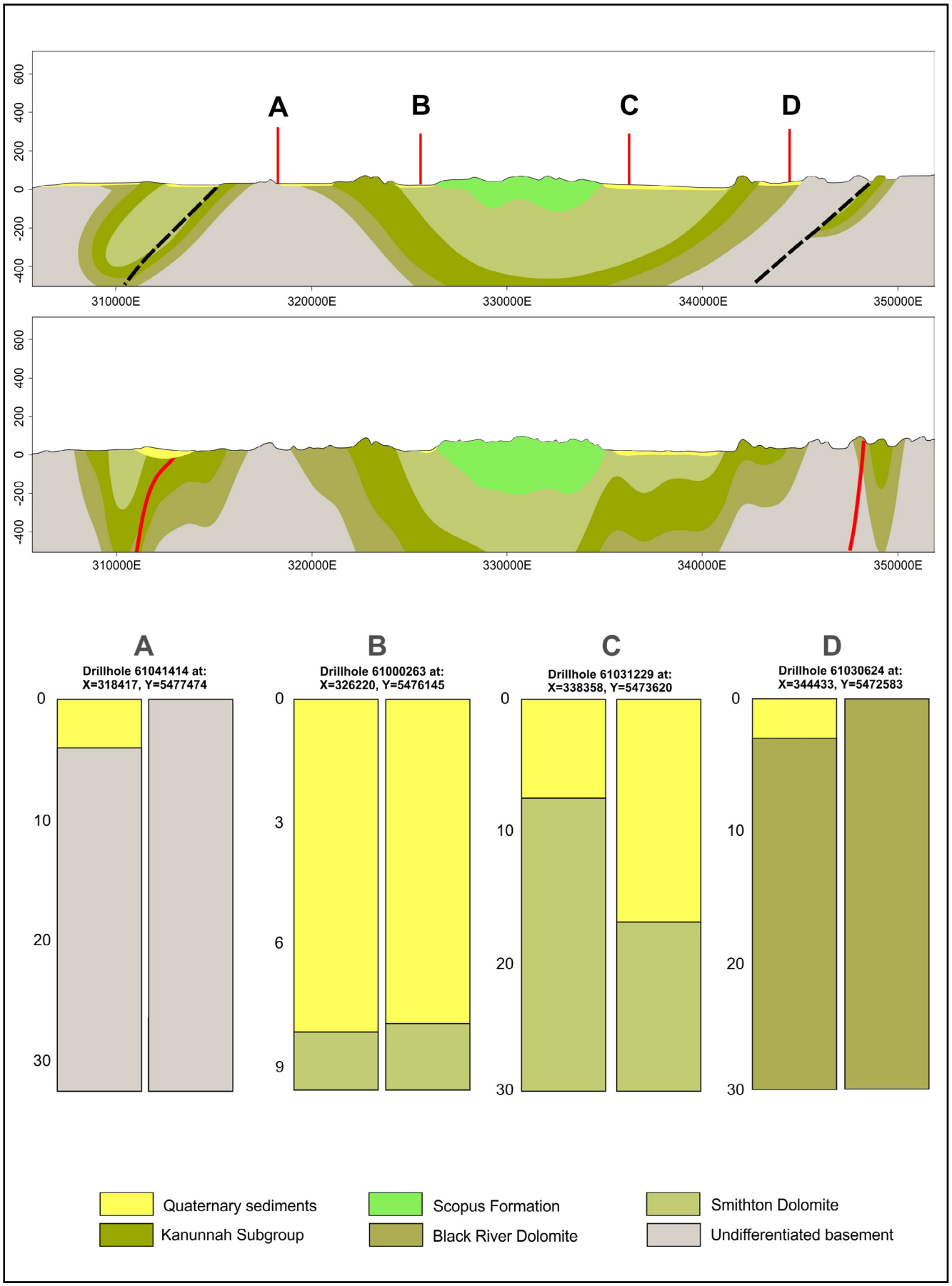

Figure 8. (Top) interpretive Section A-B Smithton Synclinorium with corresponding borehole locations denoted by A, B, C and D. Figure 8 (middle) illustrates the computed geology model. Figure 8 (bottom) shows borehole logs vs corresponding model logs.

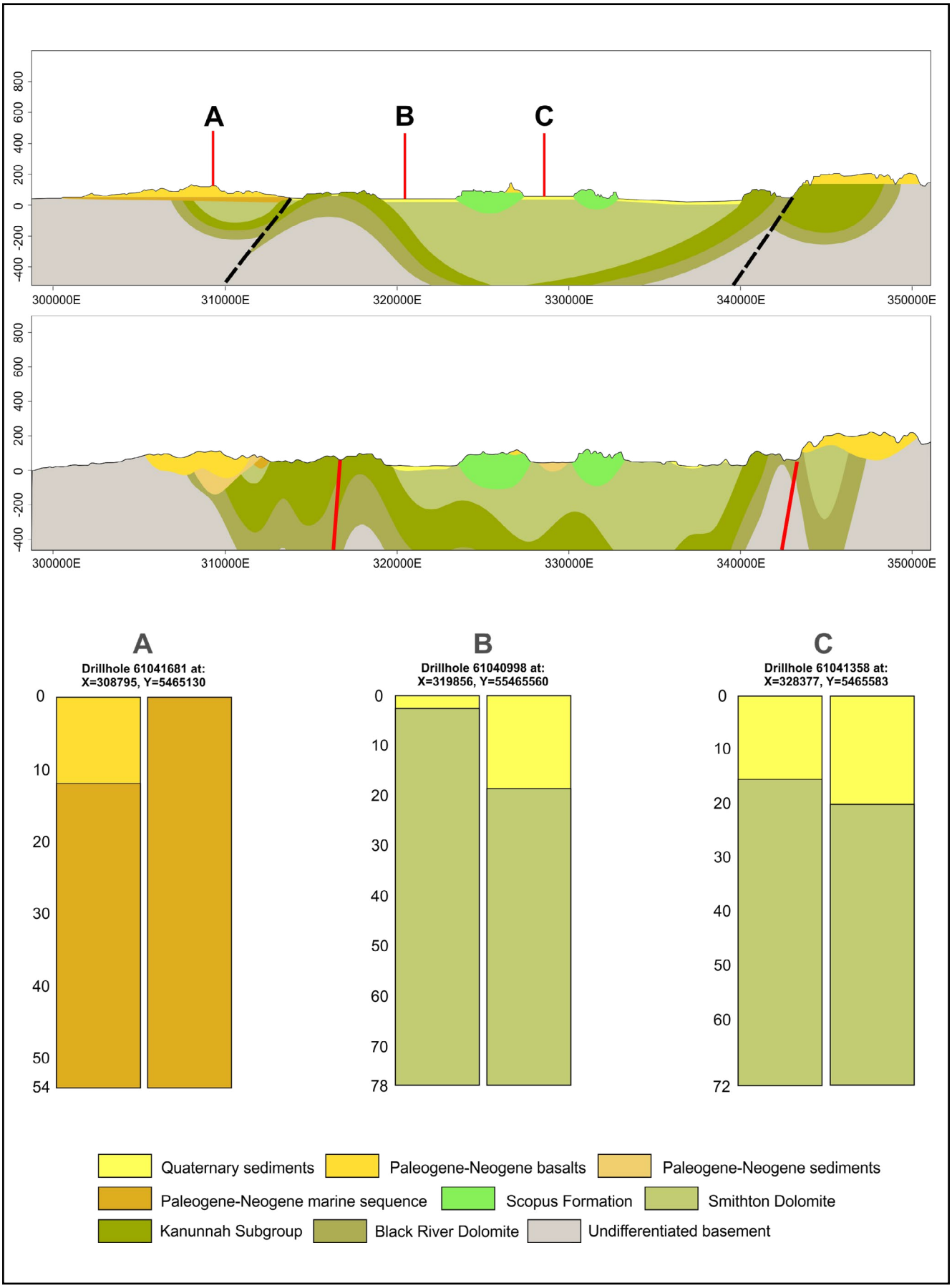

Figure 9. (Top) interpretive Section C-D Smithton Synclinorium and corresponding borehole locations denoted by A, B, C. Figure 9 (middle) illustrates the computed geology model. Figure 9 (bottom) shows borehole logs vs corresponding model logs.

along strike, with the Scopus Formation and Kanunnah Subgroup more voluminous compared to the reference sections, and the Smithton Dolomite and Quaternary sediments less so.

The Black River Dolomite is slightly more voluminous but trending thinner on the western side of the synclinorium. Upright folds towards the western end of the section are again more complex due to the use of details in Calver et al.'s (2014) sub-Cenozoic interpretation. As in Section A-B, faults (red dashed lines) are slightly steeper when compared to the reference section, as a result of re-interpretation in the course of modelling.

Differences in the Paleogene-Neogene basalt unit are also observed. The base of the basalt outcropping on the eastern edge of the computed geology section is undulating, extending up to 100 m deeper than in the reference section, where this surface is flat. This geometry is controlled by several dozen bores intercepting basalt in the area, attributable to variations in pre-basalt topographic. Details in this surface should be viewed with some caution, however, due to the uneven distribution of constraints and consequent likelihood of aliasing.

Figure 9 also illustrates the misfit between the borehole logs and computed geology model. For borehole 61041681 (A) the discrepancy is essentially spurious, the top 12 m of clays nominally assigned as Paleogene-Neogene sediment likely having affinity to the basalt shown in the model, as shown in 1:25,000 geological mapping. The model Quaternary sediment is unlikely to be as thick as shown in the vicinity of bore 61040998 (B) given all other bores in the area indicate the Quaternary as only a few metres thick. The reason for this behaviour of the model is unclear but may relate to excessive extrapolation of gradients defined in adjacent elevated areas.

The top of drillhole 61041358 (C) consists of over 15 m of clay interpreted as of Paleogene-Neogene origin. Other bores in this area contain similar material, hence the model represents the upper volume between outliers of Scopus Formation as Paleogene-Neogene sediments, rather than the Quaternary mapped at surface and shown on the reference section.

4.2 Model outputs

4.2.1 Unit grids and voxet model

The Smithton synclinorium 3D geological model volumes were converted to 2D grids, tailored for integration into hydrogeological flow models. These grids delineate the upper and lower boundaries, as well as the thicknesses, of stratigraphic layers. The model was also transformed into a voxet format, with each voxel measuring 250 m x 250 m x 10 m. This allowed for the calculation of the volumes of geological units, as illustrated in Figure 10.

Table 2 presents the volumetric and thickness data for the modelled stratigraphic units. The thickness distribution of the primary aquifer layers, comprising Quaternary deposits, Paleogene-Neogene basalts, and the Smithton and Black River Dolomites, is depicted in Figures 11a to 11d. Notably, the Quaternary deposits exhibit a maximum thickness of 284 m proximal to Smithton and in certain other isolated locations within the study area. However, these maximum thicknesses, are attributed to modelling artefacts rather than representing the observed maximum

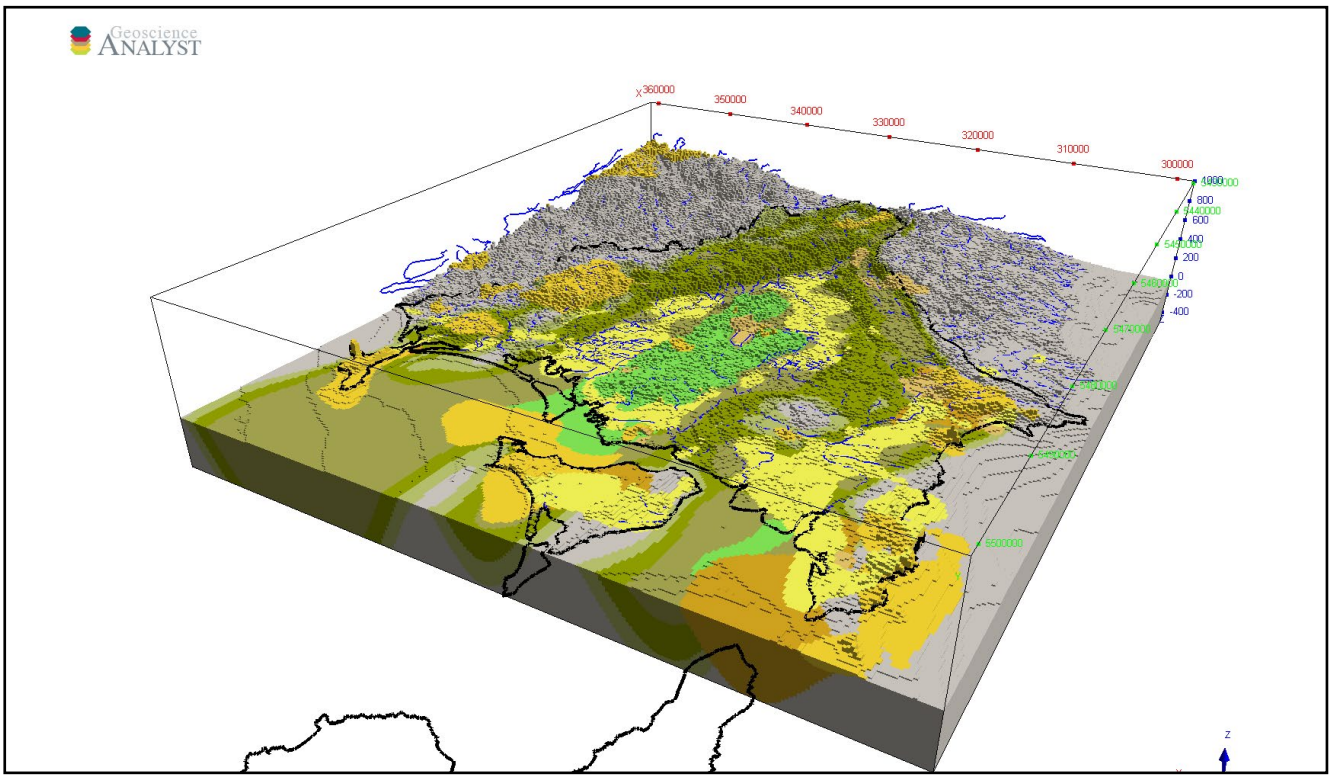

Figure 10. The Smithton Synclinorium voxet model (voxel cell size, 250 m x 250 m x 10 m) used for volumetric calculations.

Lithostratigraphy	Volume	Thickness (m)		
	km³	Average	Median	Maximum
Quaternary Sediments - Qha (note ≤ 30metres)	NA	16.9	16.8	30
Paleogene Neogene basaltic rocks - Tb	28.3	64	42.9	335.9
Paleogene Neogene marine sequence - Tm	23	150.1	121.6	495.3
Paleogene Neogene sequence sediments - Tsgs	2.7	43	37.8	226.1
Scopus Formation - Cm	76	238.6	215.2	594.1
Smithton Dolomite - Lsd	312	270.6	260.9	627.3
Kanunnah Subgroub - Lsvw, Lsv, Lsb	376.4	223.9	233.8	638.3
Black River Dolomite - Lss, Lscb	296	198.3	206.7	557.7
Rocky Cape Group - Lrj, Lri, Lrd, Lrc, Lrb, Lrl, Lrp	1,503	500	514.7	1,036.6

Table 2. (Left) Volumetric data derived from voxet lithology model and thickness variations derived from implicit modelling.

Figure 11. (Below) a) Raster grid illustrating Cenozoic Quaternary sediments thickness; b) Paleogene and Neogene basalt thickness; c) raster grid illustrating Neo-Proterozoic Smithton Dolomite thickness; and d) Black River Dolomite thickness.

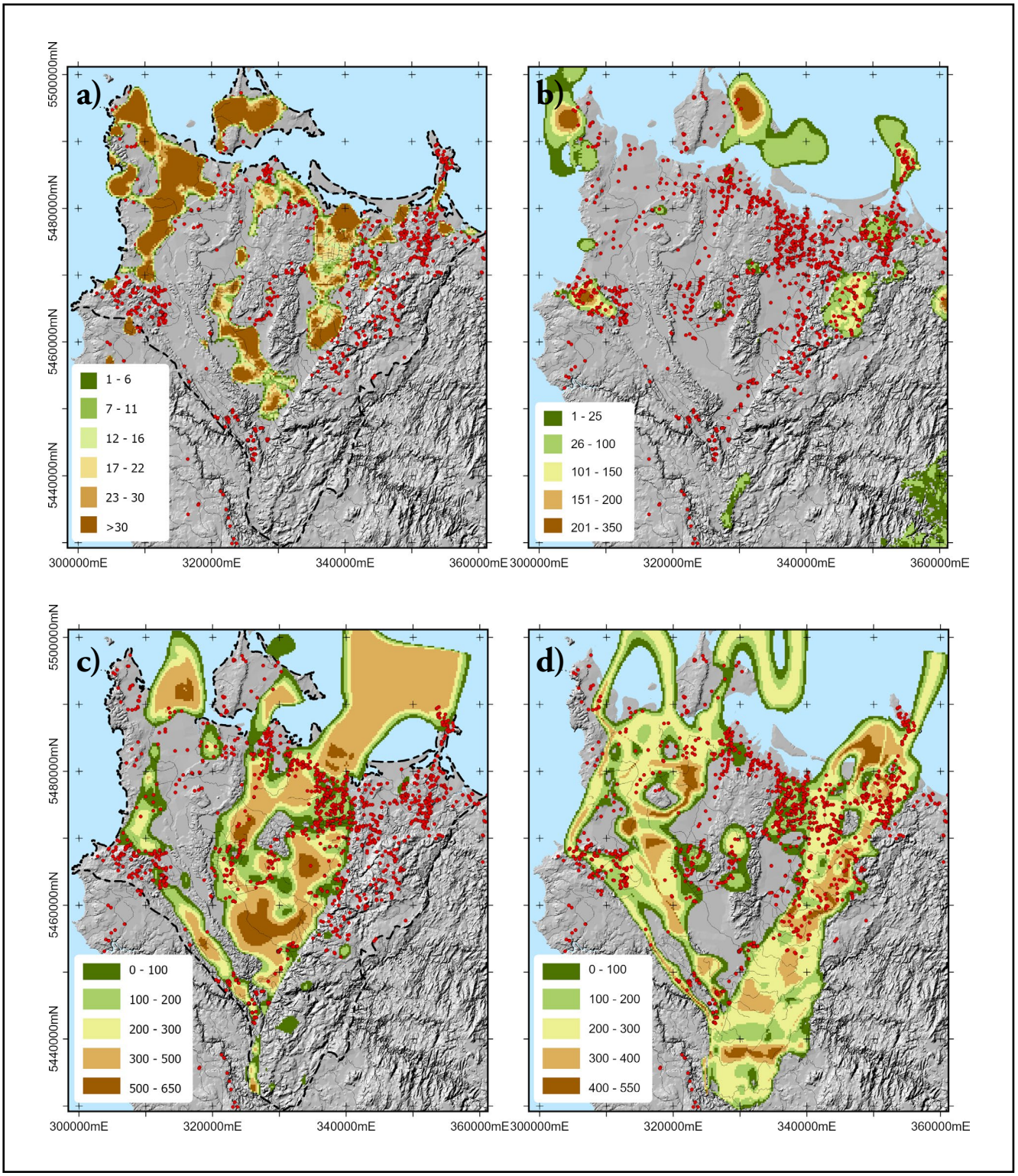

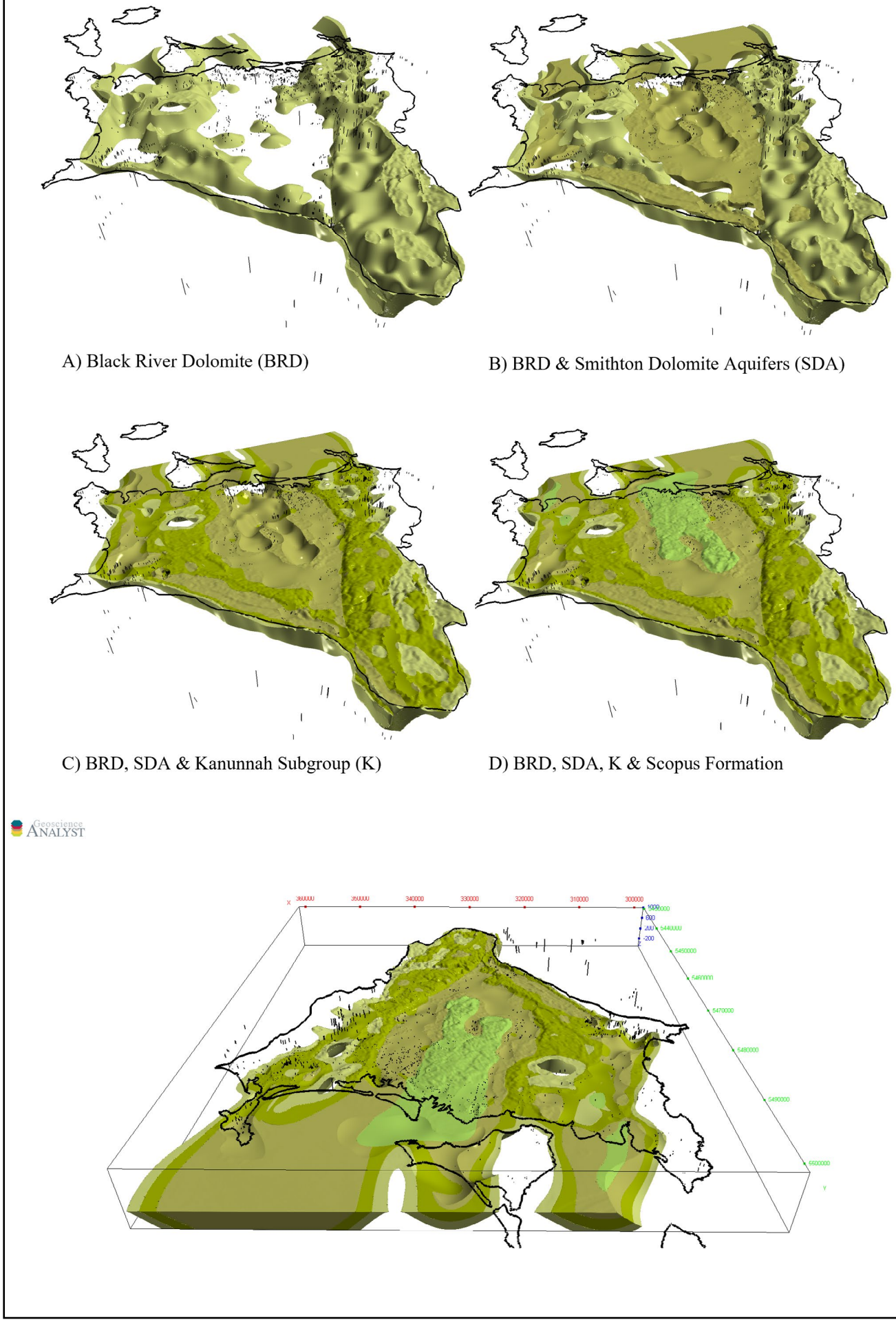

Figure 12. a) to e) illustrate the three-dimensional spatial relationship between Neoproterozoic dolomites and the Kanunnah Subgroup across the Smithton GAU catchment area.

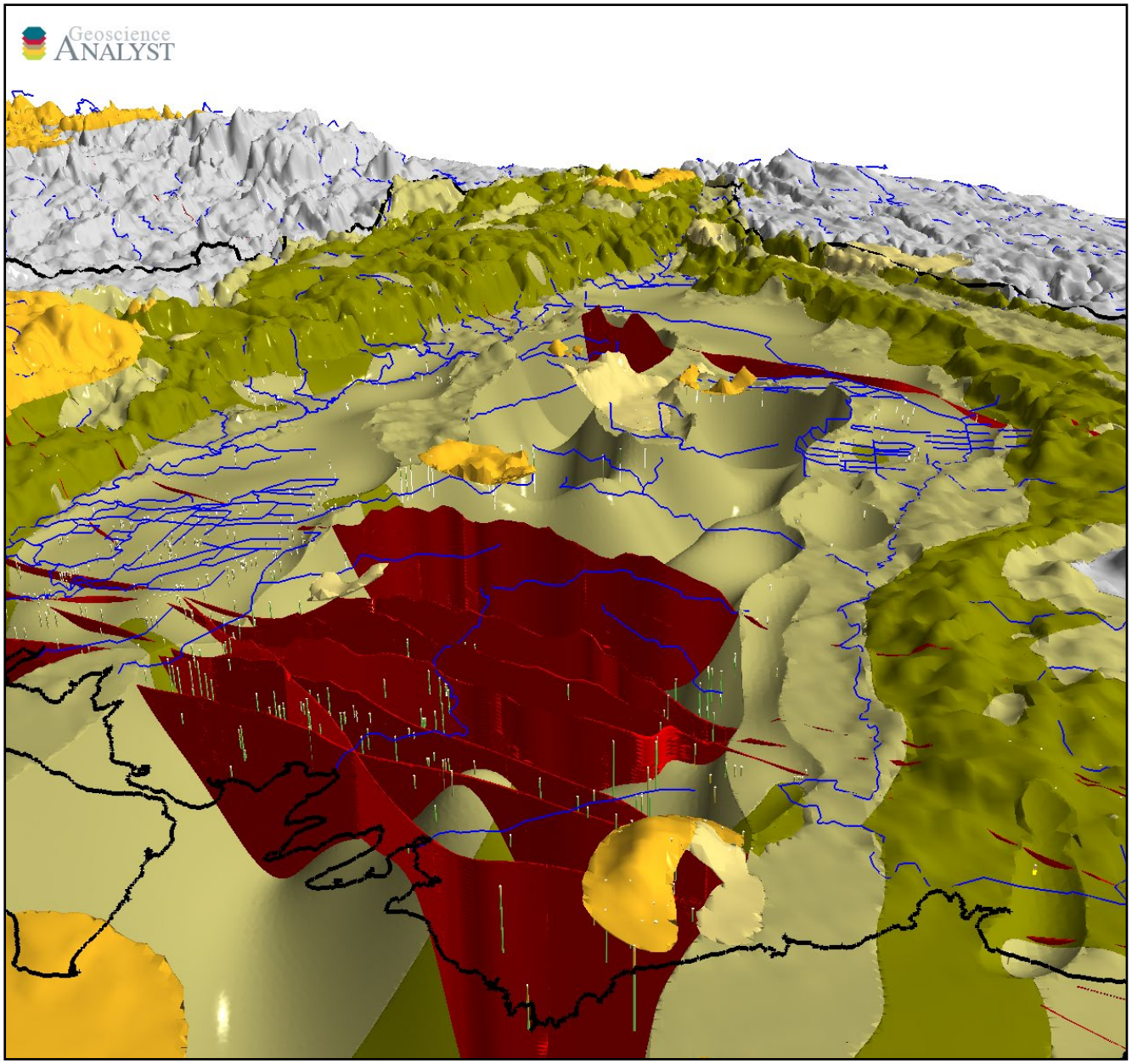

Figure 13. Dyke architecture are indicated by red surfaces. Boreholes are shown as small vertical multicoloured lines. The important aquifer host lithologies (i.e., the Smithton and Black River dolomites including the Kanunnah Subgroup) are shown as volumetric surfaces.

thicknesses of this unit, which is not more than 30 m. Therefore, a revised grid, depicted in Figure 11a, has been constructed to more accurately delineate the thickness of the Quaternary deposits, ensuring they do not exceed 30 m.

Figures 12a to 12e illustrate the three-dimensional spatial relationship between these Neoproterozoic dolomites and the Kanunnah subgroup across the Smithton GAU catchment area. The calculated volumes of these units are shown in Table 2. The Kanunnah Subgroup serves a dual role as an aquifer and an aquitard, owing to its composition of permeable sedimentary strata interspersed with impermeable basaltic layers. The volumes indicated by this study suggest that the Kanunnah Subgroup may constitute a substantial additional groundwater reservoir or conduit.

Zones of further groundwater resource potential are identified in locales where suitable formations are accessible via shallow drilling methods. Such regions include the lower segments of the Arthur-Welcome and Arthur-Roger River catchments, in addition to the northeastern periphery of the Smithton GAU, as shown in Figure 7, after DPIPWE (2014).

Figure 13 foregrounds the Mella locality, towards the northern extent of the study area. It is characterised by a significant cluster of water bores. These bores exhibit a close association with WNW-ESE-striking Cretaceous dykes, the presence of which is predominantly inferred from magnetic survey data (Figure 3). The figure illustrates how these dykes function as barriers to the northward progression of groundwater within the Smithton Dolomite. This gives rise to artesian flows and the emergence of mound springs in the vicinity.

5.0 CONCLUSIONS

The implicit modelling approach has been largely successful in characterising hydrogeological unit volumes that are consistent with geological mapping and borehole intersections. Derivatives from the model representing these units, such as grids representing their tops, bases and thickness, and discretised 3D voxets, can thus be used in subsequent quantitative groundwater analysis and modelling with a degree of confidence.

However, aspects of Quaternary sediment modelling were less successful, with excessive thickness estimates in isolated pockets of sparse data. These probably arise from ill-conditioned extrapolation of fine-scale constraint variations near the limit of vertical resolution, to the broad scale of the model.

The model enables estimation of the volume of units that act as significant aquifers and thus, when coupled with porosity information, potential groundwater capacity. The Smithton Dolomite and Black River Dolomite are inferred to have the greatest potential, with a combined volume of ~550 km^3 within the model space.

An advantage of the implicit approach taken to 3D modelling is the ability to quickly update the model in light of evolving geological information, such as might be obtained from geophysical surveys.

Conductivity imaging by airborne electromagnetic surveys would deliver insight into the likely quality of groundwater in addition to its geometry and quantity. This would be complemented by passive seismic surveys that would, suitably specified, better map both the depth of unconsolidated cover and volumes of cavernous porosity development within the major carbonate aquifers.

6.0 REFERENCES

Beaman, R. J. 2022. *High-resolution depth model for the Bass Strait - 30 m*. Geoscience Australia, Canberra.

Bombardieri, D., Denwer, K., Duffett, D., Green, G., Murphy F. C., Keele, R. A., Stapleton, P., Korsch, R. and Seymour, D. 2023. https://www.stategrowth.tas.gov.au/mrt/products/database_searches/other_searches/3d_model_data

Bombardieri, D. and Duffett, M. 2023. Statewide 3D model: Explanatory notes. *Geological Survey Technical Report,* 40. Mineral Resources Tasmania.

Brown, A. V. 1989. (comp.). Geological Atlas 1:50,000 Series. Sheet 21 (7916S). *Smithton*. Explanatory Report, Geological Survey Tasmania.

Calver, C. R. 1998. Isotope stratigraphy of the Neoproterozoic Togari Group, Tasmania. *Australian Journal of Earth Sciences*, 45, 865–874.

Calver, C. R., Corbett, K. D., Cumming, G. V., Everard, J. L., Goscombe, B. D., Jackman, C. J., Pemberton, J., Seymour, D. B. and Vicary, M. J. (updated) 2023. *Geology of Northwest Tasmania*. Edition 2023.1. Digital Geological Atlas 1:250,000 Scale Series. Mineral Resources Tasmania.

Calver, C. R., Everard, J. L., Berry, R. F., Bottrill, R. S. and Seymour, D. B. 2014. Cambrian Tasmania. In: Corbett, K. D., Quilty, P. G. and Calver, C. R. (Eds.), *Geological Evolution of Tasmania*. Geological Society of Australia (Tasmania Division), Hobart, TAS, 34–94, Special Publication 24.

Corbett, K. D., Berry, R. F., Everard, J. L., Calver, C. R., Crawford, A. J., Vicary, R. S. and Bottrill, R. S. 2014. Proterozoic Tasmania. In: Corbett, K. D., Quilty, P. G. and Calver, C. R. (Eds.), *Geological Evolution of Tasmania*. Geological Society of Australia (Tasmania Division), Hobart, TAS, 95–240, Special Publication 24.

Cumming, G. V., Berry, R. F., Bottrill, R. S., Armistead, S. E., Everard, J. L., Bombardeiri, D. J. and Meffre, S. 2024. Mesoproterozoic age for andalusite in the lower Rocky Cape Group, northwest Tasmania. *Australian Journal of Earth Sciences*, 71(3), 338–360. https://doi.org/10.1080/08120099.2024.2301934.

DPIPWE. 2012. Tasmanian Aquifer Framework Report. *Groundwater Management Report Series*, Report No. GW 2012/02. Water and Marine Resources Division, Department of Primary Industries, Park, Water and Environment, Hobart.

DPIPWE. 2014. Groundwater Report for the North-West Water Management Plan. *Water Assessment Hydrology Report Series*, Report No. WA 13/09 Water and Marine Resources Division, Department of Primary Industries, Parks, Water and Environment, Hobart, Tasmania.

DPIPWE. 2021. Rural Water Use Strategy. Department of Primary Industries, Parks, Water and Environment, Hobart. https://nre.tas.gov.au/water/water-legislation-policies-and-strategies/rural-water-use-strategy

Everard, J. L., Seymour, D. B. and Brown, A. V. 1996. Geological Atlas 1:50,000 Series. Sheet 27 (7915N). *Trowutta*. Explanatory Report, Geological Survey Tasmania.

Everard, J. L., Seymour, D. B., Reed, A. R., McClenaghan, M. P., Green, D. C., Calver, C. R. and Brown, A. V. 2007. Regional Geology of the Southern Smithton Synclinorium: Explanatory Report for the Roger, Sumac and Dempster 1:25,000 Map Sheets, Far Northwestern Tasmania. 1:25,000 Scale Digital *Geological Map Series Explanatory Report,* 2. Mineral Resources Tasmania, Hobart, 237.

Everard, J. L., Zwingmann, H., Duncan, D. McP., Bottrill, R. S. 2023. A Cretaceous age for an alkali dolerite dyke near Smithton, NW Tasmania, *Geological Survey Technical Report*, 36. Mineral Resources Tasmania.

Fox, J. M., McPhie, J., Carey, R. J. and Jourdan, F. 2023. Revised stratigraphy and first geochronology of the Miocene submarine volcanic succession at Kennaook/Cape Grim, northwestern Tasmania, *Australian Journal of Earth Sciences*, 70:4, 510-534, DOI:10.1080/08120099.2023.2181870.

Gee, R. D. 1971. ER8016S0 Geological Atlas, 1 Mile Series, Zone 7, Sheet 22 (8016S) *Table Cape*. Geological Survey Tasmania.

Gulline A. B. 1959. UGWSP5 *The Underground Water Resources of the Smithton District*. Mines Department Tasmania.

Halpin, J. A., Jensen, T., McGoldrick, P., Meffre, S., Berry, R. F., Everard, J. L., Calver, C. R.,Thompson, J., Goemann, K. and Whittaker, J. M., 2014. Authigenic monazite and detrital zircon dating from the Proterozoic Rocky Cape Group, Tasmania: links to the Belt-Purcell Supergroup, North America. *Precambrian Research*, 250, 50–67.

Harrington, G. 2008. *Conceptual model report for Smithton Syncline GMU,* REM & Aquaterra, Department Of Primary Industries, Parks, Water And Environment, Hobart.

Harrington, G. and Currie, D. 2008a. *Conceptual model report for Mella*, REM & Aquaterra, Department Of Primary Industries, Parks, Water And Environment, Hobart.

Harrington, G. and Currie, D. 2008b. *Conceptual model report for Togari*, REM & Aquaterra, Department Of Primary Industries, Parks, Water And Environment, Hobart.

Harrington, G. A., Crosbie, R., Marvanek, S., McCallum, J., Currie, D., Richardson, S., Waclawik, V., Anders, L., Georgiou, J., Middlemis, H., and Bond K. 2009. *Groundwater assessment and modelling for Tasmania*. A report to the Australian Government from the CSIRO Tasmania Sustainable Yields Project CSIRO Water for a Healthy Country Flagship Australia.

Matthews, W. L. and Donaldson, R. C. 1999. *Groundwater Prospectivity Map of Tasmania*, 1:500,000 Map (updated in 2002 by Latinovic). Mineral Resources Tasmania.

Matthews, W. L. and Latinovic, M. 2006a. 1:250,000 Groundwater Map of North-West Tasmania (groundwater prospectivity and groundwater quality maps). Mineral Resources Tasmania.

Matthews, W. L. and Latinovic, M. 2006b. Municipal Groundwater Planning Information Series Maps; 1:100,000 scale maps No 3 4 8 and 9 Mineral Resources Tasmania.

McInerney, P., Guillen, A., Courrioux, G., Calcagno, P. and Lees, T. 2005. Building 3D Geological Models Directly from the Data? A New Approach Applied to Broken Hill, Australia, *Digital Mapping Techniques '05—Workshop Proceedings*, U.S. Geological Survey Open-File Report 2005-1428

Mulder, J. A., Halpin, J. A., and Daczko, N. R. 2015. Mesoproterozoic Tasmania: Witness to the East Antarctica-Laurentia connection within Nuna, *Geology*, 43(9), 759-762.

Mulder, J. A., Everard, J. L., Cumming, G. V., Meffre, S., Bottrill, R. S., Merdith, A. S., Halpin, J. A., McNeill, A. W. and Cawood, P. A., 2020. Neoproterozoic opening of the Pacific Ocean recorded by multistage rifting in Tasmania, Australia. *Earth-Science Reviews,* 201, 103041.

Murphy, B., Denwer, K., Keele, R., Stapleton, P. Korsch, R., Seymour, D. and Green, G. 2004. Tasmania Mineral Province Geoscientific database, 3D Geological Modeling: Mines and Mineral Prospectivity Project T3, Mineral Resources Tasmania, unpublished.

Niccoli, M. 2014. How to evaluate and compare color maps, Geophysical tutorial, *The Leading Edge*, 33, no. 8, 910-912.

NRE Tas. 2024. *Groundwater Risk Assessment Tool and Management Framework*, Groundwater Assessment Project, Department of Natural Resources and Environment Tasmania.

Quilty, P. G. 1972. The biostratigraphy of the Tasmanian. marine Tertiary, *Papers and Proceedings Royal Society of Tasmania,* 106, 25–44.

Seymour, D. B. 1997. A re-evaluation of the structural significance of the Boat Harbour Fault, northwestern Tasmania. *Tasmanian Geological Survey Record,* 1997/09.

Stadder, M. 2009. Model Calibration and Prediction for Mella Togari. REM & Aquaterra, Department Of Primary Industries, Parks, Water And Environment, Hobart.

Rockliff, D. and Sheldon, R. 2011. *Smithton Syncline Groundwater Management Area: Hydrogeology Groundwater and Surface Water Connectivity*, Water and Marine Resources Division Department of Primary Industries Parks Water and Environment, Hobart.

APPENDIX

Model Products

Data format and visualization

The model is being distributed as a Geoscience ANALYST project and is described here as such. Geoscience ANALYST is visualisation and communication software for GoCAD® 3D models, made freely available by Mira Geoscience(http://www.mirageoscience.com/).

All spatial objects within the model are referenced to the GDA 94 Datum.

1) Digital Elevation Model (DEM)

Onshore and offshore surface topography of the Smithton Basin was extracted from the high-resolution depth model for Bass Strait - 30 m. Geoscience Australia, Canberra. Digital elevation model resampled to 120 metre cells.

https://dx.doi.org/10.26186/147043

2) Drillholes

Collar and hole geometry for the 1,080 holes from GWIMS and 372 for TIGER were recorded on open file for the study area. These drillholes were attributed with downhole information which includes the stratigraphic unit or lithology intersected.

Fault surfaces are interpreted from surface mapping and cross sections. Most are named, some in line with established local practice, others for the first time in the course of model construction.

3) Raster grids

3.1 Geology 1:250,000

Geological map extracted from published MRT 1:250 000 series, which should be referred to for legend information.

3.2 Lithology base

3.3 Lithology tops

3.4 Lithology thickness

3.5 Total Magnetic Intensity

The TMI grid, containing values in nT after subtraction of the International Geomagnetic Reference Field, was generated with a mesh size of 40 m and has been coloured with the 'cube' perceptually balanced palette of Niccoli (2014). The magnetic grid is a stitch of various TMI surveys flown between 1957 and 2022 with line spacings varying between 50 m and 1,500 m.

4) Vectors

Vector files include dykes, rivers and structural measurements from 1:25,000 scale mapping. Tasmanian coastline, faults and lithology are sourced from 1:250,000 scale mapping.

5) Volumetric Surfaces

Surfaces bounding unit volumes were interpolated from geological observations (stratigraphic and fault contacts, dips, and strikes) via prior geological knowledge encoded in a matrix of rules defining the relative timing of all model components.

6) Voxet model

Discretised 3D voxel (cell) representation (250 m x 250 m x 10 m) of the geology used for volumetric calculations.

Tasmanian Government

Mineral Resources Tasmania
PO Box 56 Rosny Park
Tasmania Australia 7018
Ph: +61 3 6165 4800

info@mrt.tas.gov.au www.mrt.tas.gov.au